2014

Revisiting the carousel and non-radial oscillation models for pulsar B0809+74

Joanna Rankin

Rachel Rosen

Monthly Notices
of the
ROYAL ASTRONOMICAL SOCIETY

MNRAS **439,** 3860–3867 (2014)
Advance Access publication 2014 March 3

doi:10.1093/mnras/stu237

Revisiting the carousel and non-radial oscillation models for pulsar B0809+74

Joanna Rankin[1,2]★ and Rachel Rosen[3,4]

[1]*Physics Department, University of Vermont, Burlington, VT 05405, USA*
[2]*Sterrenkundig Instituut 'Anton Pannekoek', University of Amsterdam, NL-1090 GE Amsterdam, the Netherlands*
[3]*National Radio Astronomy Observatory, Charlottesville, VA 22091, USA*
[4]*West Virginia University, White Hall, Morgantown, WV 26506, USA*

Accepted 2014 January 31. Received 2014 January 23; in original form 2013 November 19

ABSTRACT

Recent interest in pulsar B0809+74, well known for its highly accurate drifting subpulses and 'memory across nulls' has raised questions about the adequacy of the rotating subbeam-carousel or/and non-radial oscillation models to describe this phenomenon. The success of the subbeam-carousel model in explaining the drift modes and periodic nulls in B1918+19 has encouraged us to revisit the application of this model to B0809+74. Pulsar B0809+74 is a complicated object, as are many pulsars where our sightline grazes the conal beam edge obliquely. Its subpulses also exhibit complex modal polarization, and only analysing the total power paints an incomplete picture of emission from the star. This remarkable pulsar has, however, been studied in great detail for over three decades, and many of the earlier controversies about its characteristics have largely been resolved. In this paper, we demonstrate that the carousel model is highly successful in reproducing the behaviour of B0809+74 in every heuristic and geometric manner. In addition, Rosen and Demorest have quantitatively fitted a non-radial oscillation model to B0809+74 at a single frequency, and we discuss how this model can reproduce the behaviour of B0809+74 across a much larger band.

Key words: methods: analytical – techniques polarimetric – pulsars: general – pulsars: individual: B0809+74.

1 INTRODUCTION

Radio pulsar B0809+74 is well known for its bright and precisely drifting subpulses, which have an unusually large driftband spacing (P_3) of 11 rotation periods (P_1) and also for its exceedingly broad spectrum. It has been observed down to approximately 10 MHz and up to around 10 GHz, and unusually its spectrum hardly turns over at low frequency.

Remarkable new possibilities for acquiring high-quality low-frequency observations (e.g. Hassell et al. 2012a,b, hereafter Hassall I/II, respectively) have revived interest in various aspects of this pulsar's emission and subsequent interpretation. The phenomenology of B0809+74's emission has proven to be quite complex, but many of the earlier controversies regarding its basic emission characteristics have by now largely been resolved. In particular the following discussed below.

1.1 Grazing sightline traverse

Every known well-studied pulsar with broadly drifting subpulses has a sightline that just grazes the emission cone tangentially. This makes sense geometrically, and models of the basic emission geometry also bear it out. Such pulsars are denoted as conal single ($\mathbf{S}_d$) or in some other cases as conal triple (c$\boldsymbol{T}$) in the classification schema of the 'Empirical Theory' (Rankin 1993, hereafter ET VI) and entail a ratio β/ρ of typically $\sim|0.8|$ or more (where β is the sightline impact angle and ρ is the conal radius out to the outside half-power point). Lyne & Manchester's (1988, hereafter LM) work reaches very similar conclusions.

The conclusion that pulsars with well-organized drifting subpulses have a geometry where the sightline tangentially grazes the emission cone is also consistent with a non-radial oscillation model. Clemens & Rosen (2004) show, in fig. 3 of their paper, that the absence of a nodal line, such as in a conal geometry, leads to organized drifting subpulses. However, if a nodal line is present, which would include some (but not all) double profiles, the nodal line modulates the subpulses and creates more complex behaviour.

1.2 Conal spreading at low frequency

Strong evidence suggests (e.g. ET VI) that emission cones appear to increase in angular size systematically with wavelength. This phenomenon has become known as 'radius-to-frequency mapping' (e.g. Cordes 1978). However, the physical causes remain

★E-mail: Joanna.Rankin@uvm.edu

uncertain. The received notion is that the emission height increases as the plasma frequency decreases, but refraction might also play a strong role (e.g. Lyubarski 2008). Outer cone widths escalate faster than those of inner cones, and in some cases the latter remain fairly constant. This differential behaviour is very clear and consistent in stars with double cone/core profiles such as B1237+25 (again see ET VI). Further, the Thorsett (1991) model provides a very adequate empirical relationship for conal spreading at low frequency. In short, conal spreading is a usual and expected effect that must be accommodated in understanding drifting subpulses at lower frequencies. B0809+74 appears to exhibit the effect strongly below 100 MHz.

1.3 Incomplete profiles

In addition, most pulsars with grazing sightlines have profiles that are incomplete, or 'absorbed' – often at metre wavelengths – that is, their widths are not as large as would be expected when extrapolating from lower frequency where the cone size is apparently larger and the emission extends roughly over the full angular width of the polar cap. Or, equivalently, that single-pulse correlation techniques show that an incomplete profile corresponds to only a part of a more complete one at some other frequency. It is not fully clear why this is so, but there are several obvious and probable reasons:

(i) the conal edge is not smooth or even jagged as in the Deutsch (1955) or other conal beam models,

(ii) because the sightline traverse is so shallow that it never penetrates as far as the radial peak and is thus incommensurate with the dimensions of lower frequency profiles where it does,

(iii) the emission mechanism is itself asymmetric about the longitude of the magnetic axis for a host of possible reasons (intrinsic strength, degree of coherence, aberration/retardation, etc.)

(iv) or perhaps because there is actual physical absorption (or scattering) above a part of the polar cap. Indeed, given the huge magnetic field and dense plasma in the inner magnetosphere, it is difficult to understand theoretically how the radio-frequency absorption could be less than total (i.e. Lyubarski 2008)!

Therefore, B0809+74 is typically and expectedly complex in this regard compared to other well-studied pulsars with profiles reflecting grazing sightlines. And this complexity associated with incomplete profiles seems to occur primarily at metre or higher frequencies where the sightline traverses are often shallower than expected. Another well-known drifter, B0943+10, shows time variability in the completeness of its B-mode profile after onset (Rankin & Suleymanova 2006). ET VI found that geometrical models could not be as precise for $\mathbf{S}_d$ stars because of the above. Mitra & Rankin (2011, hereafter ET IX) found that many of LM's 'partial cones' are in fact conal single pulsars with incomplete profiles stemming from grazing sightlines.

Incomplete profiles, aka 'absorption' (note the quotes), are a matter of observable fact – and not uncommon among the normal pulsar population. Parts of B0809+74's profiles are missing at certain frequencies, and we cannot yet be fully sure which profiles and frequencies are affected. Single-pulse correlations between certain bands show this clearly. For instance, when 380-MHz pulses are correlated against their 1400-MHz counterparts, we see that the drifting subpulses in the leading part of the latter have no counterparts in the former – whereas those in the trailing part of the profile do (e.g. Rankin, Ramachandran & Suleymanova 2006a, hereafter Paper 1: fig. 4).

'Absorption' is thus not a theoretical interpretation, it is an observationally demonstrable effect. Bartel et al. (1981; also Bartel 1981) named it – perhaps poorly – and when low-frequency profile alignments were compared for B0809+74, it produced the appearance of 'superdispersion' (e.g. Shitov & Malofeev 1985). While the physical process behind 'absorption' is poorly understood, the observable effects are well documented.

1.4 Depolarized conal edges

The edges of conal beams corresponding roughly to the 'last open field lines' of the polar flux tube are virtually always highly depolarized (Rankin & Ramachandran 2003). This edge depolarization is an important characteristic of conal beams and appears to result from the circumstance that the two orthogonal polarization modes (OPMs) have comparable strengths on the outer edges of cones. In pulsars with regular subpulse modulation, this edge depolarization is produced by sets of primary and secondary polarization mode (PPM and SPM) 'beamlets' or subpulses offset from each other by about 180° in modulation phase.

Conversely, such edge depolarization provides a reliable means of identifying the edges of cones. B0809+74's high-frequency profiles show no such edge depolarization on one or both wings of their profiles, whereas its lower frequency profiles show ever more. Indeed, the leading edges of the pulsar's profiles at 1 GHz and above are nearly unique in exhibiting almost complete linear polarization; such high linear polarization is very rare in conal profiles and indicates that the sightline is encountering a single fully polarized OPM in this region.

1.5 Dynamic profile structure

The concept of a pulsar 'component' is a bit fuzzy at best. However, in many cases it is the intensity-weighted distribution function of subpulses that accrues almost randomly within a restricted region of longitude. Therefore, we can talk meaningfully about the structures of pulsars with two, three or even five components whose widths are relatively narrow compared to the overall profile width.

However, conal single profiles are not like pulsars with multiple components. Rather, they aggregate the emission from individual subpulses that often *systematically* drift through them. Various geometrical and physical factors contribute to the intensity level at different longitudes, so there will be little clear meaning to a peak or to some combination of constituent Gaussian forms.

1.6 Multifrequency profile alignment

The common method of aligning pulsar profiles across many frequencies is to use the known dispersion such that similar instants at different frequencies are placed on a common basis – as if we were observing in the immediate vicinity of the pulsar. Conversely, short-duration broad-band effects can be used to determine the dispersion as did Bruk et al. (1986) for B0809+74 at low frequencies using microstructure.

Using dispersion alignment, conal profile centres align closely – as long as they are complete – for instance, as evidenced by their depolarized edges. B0809+74's higher frequency incomplete profiles can then be aligned only by dispersion – that is, similarly to those seen in Fig. 1.

However, it is problematic on several grounds to use B0809+74's profiles of themselves to establish a reliable alignment, because some of the profiles are incomplete. The proper methodology is

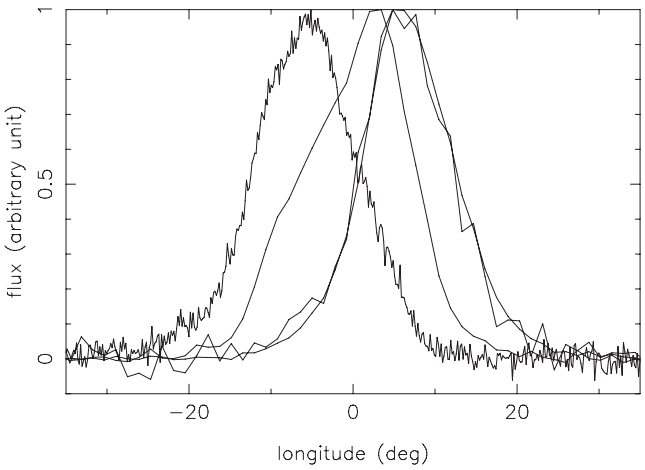

Figure 1. A display of profiles at 382 (rightmost profiles), 1375 (centre profile) and 4880 MHz (left-hand profile) assembled to explore the high-frequency alignment from Paper 1 (see this paper for details). Apparently, none of the pulsar's profiles in the centimetre-wavelength region have edges that align in a simple manner.

to align not the profiles but the constituent subpulses and/or microstructure (to the extent possible given conal spreading at low frequency).

1.7 Basic emission geometry

Geometric models using both profile width and polarization provide reasonably accurate and consistent basic emission configurations – that is, the magnetic latitudes α and sightline impact angles β, though for most pulsars it is difficult to determine whether β is positive (equatorward) or negative (poleward). For B0809+74, α is about 9° and β ±5° (see Paper 1: tables 2 and 3).

1.8 Drifting subpulse 'phase jumps'

Discontinuities in the modulation phase ('phase jumps') of drifting subpulses near the centres of certain profiles are common. They can occur when either (a) incommensurate intervals of magnetic and rotational phase accrue between leading and trailing portions of a profile or (b) the two parts of the pulse profile (leading and trailing) have different OPMs. In these situations, a roughly 180° modulation-phase 'jump' will occur at the boundary.

These effects are seen in a few different pulsars and the OPM-related 'jumps' are readily understood within the carousel model when they are analysed polarimetrically. Several examples of such effects are shown in Rankin, Ramachandran & Suleymanova (2005, hereafter Paper 0: figs 5 and 6); however, we now see that the graphical presentation was not completely clear. We give here revised versions of these modulation-folded displays in Figs 2 and 3, that show *both* the total power (contours) and modal polarization (colour scale) behaviour of the driftbands.

2 REVISITING B0809+74'S CAROUSEL MODEL

2.1 Dispersion alignment

A rotating subbeam-carousel model for B0809+74 makes no physical sense unless we view each member 'beamlet' of such a system as potentially radiating over the entire radio-frequency spectrum. This in turn requires that the observations in each band be aligned, in principle, such that a polarized beamlet momentarily passing the central longitude (of the magnetic axis) be simultaneous – and note that the central longitude does not necessarily mean the centre of the pulse profile, as discussed in Section 1.3. This is the dispersion alignment which was determined accurately and at very low frequency by Smirnova et al. (1986) to entail a dispersion measure (DM) of 5.751 ± 0.003 pc cm^{-3} [see also Bruk et al. (1986) and Popov, Smirnova & Soglasnov (1987)]. Various earlier analyses were made to determine how B0809+74's high-frequency emission aligned using single-pulse cross-correlations (e.g. Page 1973). These efforts of course drew on observations far inferior to those now available (see Hassall I and II), but found the DM to be similar to that of these 25-yr old measurements. Futhermore, Bruk et al. (1986) and Popov et al. (1987) developed a robust, and still relevant, methodology of correlating measurements across multiple frequencies.

The Hassall I analysis presents a huge collection of observations and exhibits strongly the remarkable power and broad capabilities of the new LOFAR instrument. The alignment of their multifrequency profiles, however, is based on a single Gaussian-fitted component across all frequencies. This alignment technique potentially suffers from all of the issues discussed in the foregoing section, and their analysis does not address the evidence for missing portions of some profiles and consequent non-dispersive alignments encountered by earlier investigators.

This said, Hassall I appear to measure a compatible DM value of 5.75 pc cm^{-3} – not, however, by a technique that can be directly compared with the older measurements above (Hassall private communication). Given B0809+74's history and complexity, one or the other above microstructure techniques provide by far the most reliable method for aligning its profiles and subpulses. There are several issues, both with prior and current observations and analysis that need to be resolved. First, Bruk et al. do not clearly state that their value aligns the centres of their low-frequency profiles. Secondly, their measurements are now almost three decades old, and while most pulsar DM values are fairly stable in time, this should not be taken for granted. A new low-frequency microstructure determination is now certainly warranted, and this might be carried out even with existing LOFAR observations.[1] The calculation of the DM from the microstructure might be possible from the data collected by Hassall et al. (2012a,b). Thirdly, if the Bruk et al. value remains correct, and if further it aligns the profiles as depicted in fig. 11 of Hassall I, then the pulsar's profile incompleteness may be an even more serious consideration. Could it then be that B0809+74 reflects a conal triple (c***T***) configuration wherein the inner cone is visible as their aligned feature, the trailing sightline traverse through the outer cone produces their trailing component at low frequencies, and the leading outer conal component is missing over the entire long wavelength region? Were this the case, it could explain much, very possibly including some of the 'kinks' in the driftbands.

2.2 Driftband analysis

Much of the analysis in Hassall II is beautifully carried out according to the framework established in Hassall I. More than for any other pulsar, however, it is risky to undertake an analysis of B0809+74 drifting subpulses on the sole basis of total power. Indeed, there is

[1] The Hobbs et al. (2004) value of 6.116 ± 0.018 from timing seems unreliable for the present purposes.

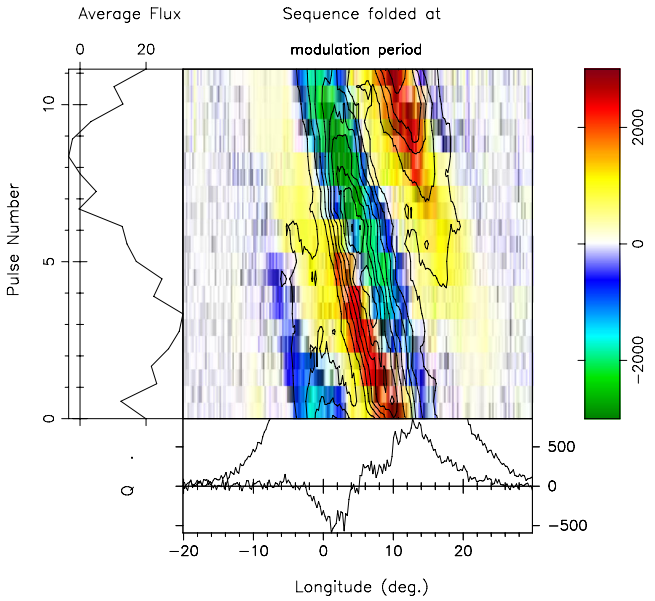

Figure 2. Folded 328-MHz driftband (top left) showing the total power (contours) and the modal polarization (colour intensity coded) in terms of the rotated Stokes parameter Q' (see Paper 0 for details). The two OPMs are coded positive and negative, and close inspection shows that the total power driftband is canted with respect to the two modal overlapping driftbands. Top right: a display of the total power modulation phase, with the profile and the modulated power in the top panel and the phase in the lower one. Bottom right: polarized profile of the same pulse sequence. The overall depolarization is striking, and one can see that the two regions of modal polarization overlap more in the leading region than the trailing.

some confusion in the early papers (reviewed in Paper 0) because the analysis only considered the total power and thus could not take into account the polarization properties of the pulsar.

The polarized subbeam maps in Rankin et al. (2006b, hereafter Paper 2: fig. 4) show why a total power analysis is incomplete for B0809+74. Similar depictions can be found in Ramachandran et al. (2002) and Edwards (2004). In this pulsar at high frequency, the PPM and SPM beams have comparable power, whereas in other pulsars, the PPM beamlets are more dominant. Note what was done here: the polarized power is rotated into a single Stokes parameter Q' so that PPM power is shown positive and SPM negative. These 10-beam maps show that the sightline cannot help but encounter both sets of OPM beamlets, generating a complex admixture that conflates, depolarizes, and alters the timing of their resulting combination.[2]

The argument in Hassall II is correct that there are two sets of overlapping driftbands at high frequency. But when one compares the corresponding panels of their fig. 5 with the polarized folded driftbands of figs 5 and 6 of Paper 0 it appears that these two driftbands correspond to the two OPMs. At 1380-MHz one, OPM is active in the early part of the profile over the entire modulation cycle, whereas both compete in the trailing region over portions of the cycle to depolarize the profile. Then, at 328 MHz, we see that the two OPMs more nearly overlap throughout the modulation cycle.

[2] Hassell I make one polarization argument in their fig. 13, and what is impressive about this figure is the broad-band character of the *depolarization*, such that little sense can be made out of the residuum.

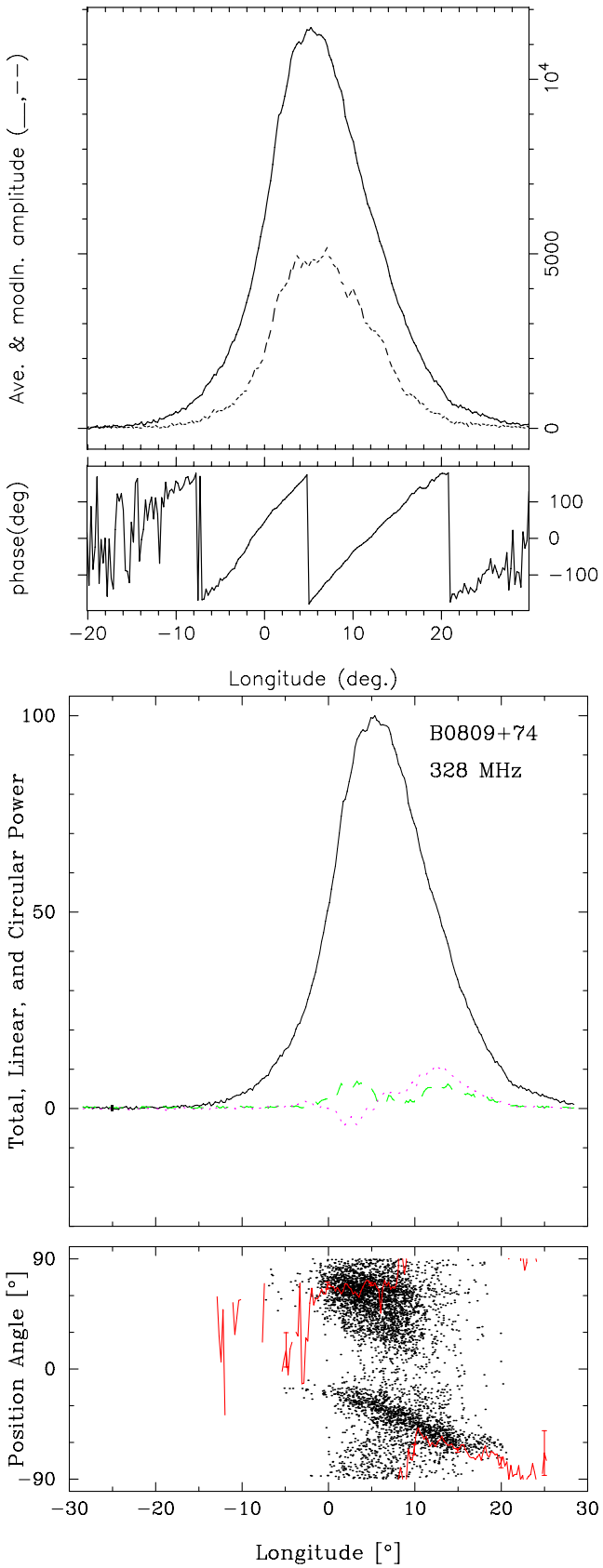

Figure 2 – *continued*

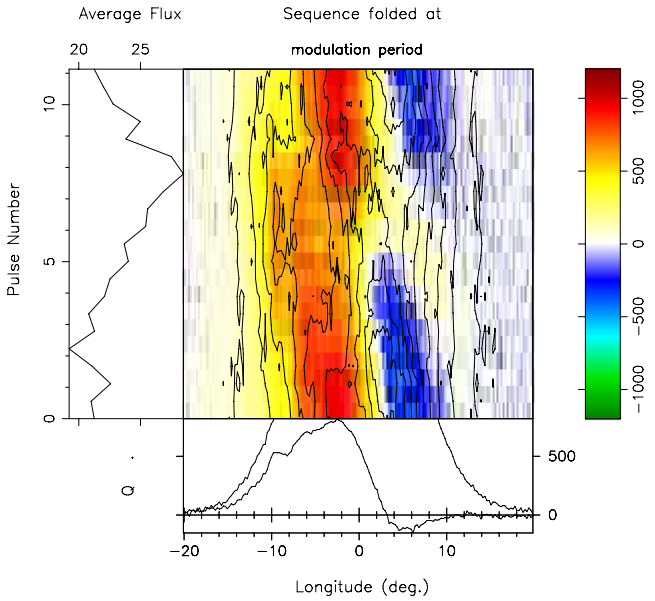

Figure 3. Folded 1380-MHz driftband (top left) showing the total power (contours) and the modal polarization (colour intensity coded) in terms of the rotated Stokes parameter Q' (see Paper 0 for details). The two OPMs are coded positive and negative, and one can see that the driftband is comprised of two different OPMs and that they change sharply in the centre of the profile. Top right: a display of the total power modulation phase, with the profile and the modulated power in the top panel and the phase in the lower one. Note the roughly 180° modulation phase change at 0° longitude associated with the OPM transition. Bottom right: polarized profile of the same pulse sequence. The contrasting large fractional linear polarization in the leading part of the profile and complete depolarization in the latter half is striking.

A problem with this analysis in Paper 0 is that the total power driftband was not shown, so a reader could not see as clearly as needed how it is that the total power and polarized driftbands behave differently. We have repaired that in Figs 2 and 3 here. At 328 MHz, the Stokes *I* driftband is somewhat canted with respect to the modal driftbands, but there is no discontinuity in modulation phase, and the two OPM driftbands almost completely depolarize the overall profile. At 1380 MHz, the situation is very different: one OPM is associated with the driftband in the early part of the profile and the other in the trailing half with a sharp transition midway. This results in the roughly 180° modulation-phase step identified by many writers. Here, very unusually, the leading part of the profile is highly linearly polarized and the trailing part highly depolarized.

What happens at lower frequencies is perhaps less of a polarization effect, but even at around 100 MHz we can see in fig. 3 of Paper 0 that the two OPMs are overlapping but such that one is much stronger in the leading and the other in the trailing portions of the profile. At decametre wavelengths, the driftbands further divide not because of polarization but because here the star's profile begins to have actual component structure due to conal spreading – dividing progressively into an apparent conal double (or one-sided c***T***) configuration.

2.3 'Frequency-dependent delay'

The depiction of B0809+74's driftbands in fig. 5 of Hassall II is very impressive in terms of both quality and extent, especially into decametre wavelengths. In no previous work is the pulsar's

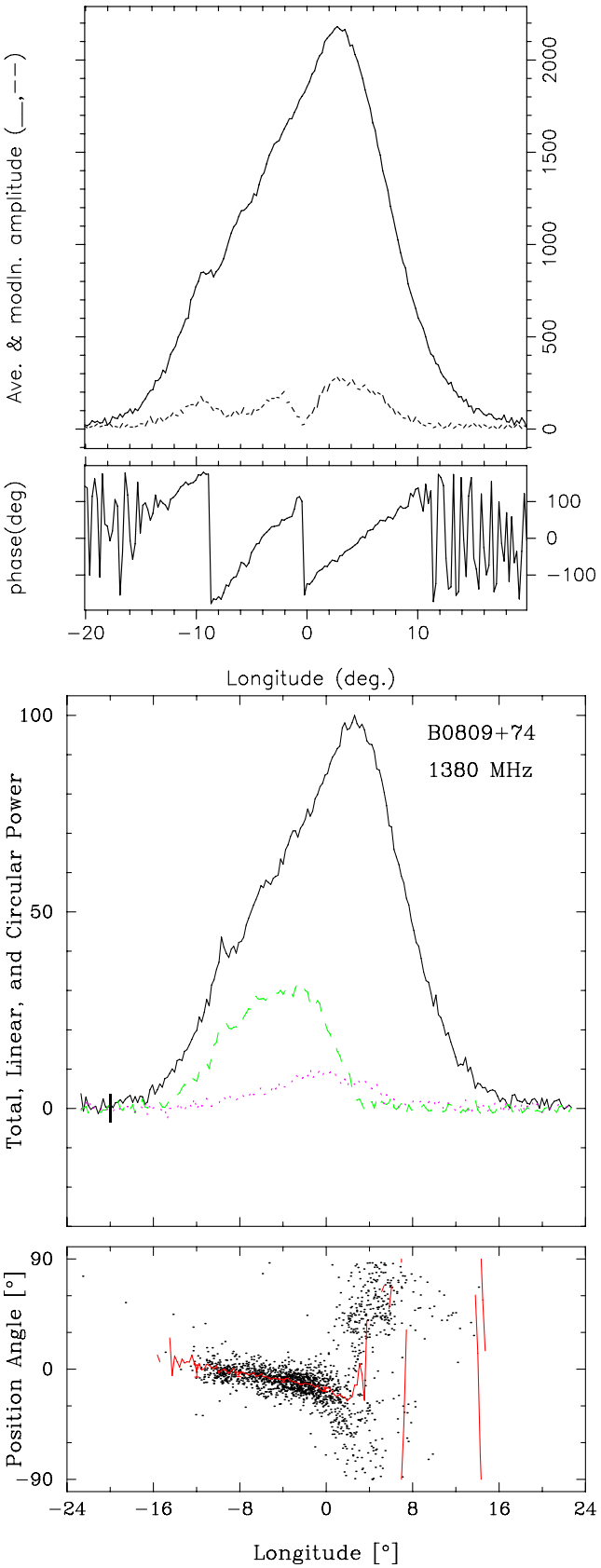

Figure 3 – *continued*

conal spreading exhibited so clearly and extensively. However, their interpretation leading to a putative 'frequency-dependent delay', stemming from the great length of the driftbands at low frequency, is flawed and incorrect.

Most use of the rotating carousel-beam model is still unfortunately more geometry than physics – all due respect to Ruderman & Sutherland (1975) notwithstanding. So, if one wishes to assess the efficacy of this model, the analysis must be conducted in the context of a full frequency-dependent geometrical model of the carousel-beam emission of the pulsar, which Hassall II did not attempt.

The carousel model expects more driftbands at low frequency compared to high frequency because of conal spreading (see Section 1.2) and that these driftbands will extend longer in longitude extent across pulse profile – and this circumstance is seen strongly in pulsar B0809+74. Fig. 5 of Hassall II shows that hardly two (or at most three) driftbands occupy the width of the profile at any frequency down to 100 MHz – and that driftbands persist for times hardly longer than the 11-P_1 P_3. At decametre wavelengths, however (for instance at 44 MHz), the number rapidly increases to some 5 at perhaps hardly an octave lower; and the bands persist for three or even most of four times P_3.

This behaviour is completely expected within the carousel model. For the same reason that the profile bifurcates into first two unresolved components and ultimately two well-resolved ones – indicating that the sightline traverse is ever more central (the cone growing while β remains constant) – the overall width of the profile spans more beamlets. Moreover, because these beamlets are regularly spaced in magnetic azimuth, the (rotationally centred) sightline arc between the edges of the profile becomes progressively shorter than the magnetic azimuth arc. This has the effect of crowding beamlets (or driftbands) into the growing width of the profiles at decametre wavelengths. (e.g. see fig. 5 of van Leeuwen et al. (2003) and consider the effects of even more central sightlines.)

For instance, in the 32-MHz panel, it takes a very long time for a particular beamlet (or subbeam) to rotate across the full width of the profile – indeed, something upwards of 40 stellar rotations. Therefore, Hassall II's 'frequency-dependent delay' actually entails rather little physical delay. Rather, it is primarily the expected rotational phase delay of the carousel. Because their analysis did not include the geometry and dynamics of the rotating carousel, they were left with no recourse but to interpret what is mostly a rotational phase delay as a physical time delay.

Therefore, the subbeam-carousel model of pulsar B0809+74's drifting subpulses remains an accurate description of the complex behaviour that this pulsar exhibits. Indeed, the characteristics of this carousel-beam system can be modelled quantitatively in substantial detail as was done in Paper 2: tables 2 and 3. Note in particular that P_2 is virtually constant down to 100 MHz and further increases slowly down to 17 MHz – and it is interesting to compare these values with the overall profile widths. Clearly, the long-wavelength profile widths grow very much faster than P_2. Note that this is true irrespective of how the high-frequency profile widths are modelled.[3]

[3] Overall, this will also be true even if the pulsar were to have an asymmetric conal triple configuration. The needed model would then, of course, be a different one, describing the subbeam delays between the inner cone and the visible (trailing) part of the outer cone, rather than between two outer cone segments. Conal spreading, however, would still be a dominant issue and quantitatively not dissimilar.

3 REVISITING B0809+74'S NON-RADIAL OSCILLATION MODEL

In a series of papers, Clemens and Rosen developed a non-radial oscillation model to describe drifting subpulses and their associated behaviour. The fundamental assumption of the model is that the neutron star is undergoing non-radial oscillations of high spherical degree (ℓ) aligned with the magnetic axis which modulate the radio emission in addition to the rotational modulation. The average pulse shape and number of components are determined by the number of latitudinal nodes contained in the polar cap. The standing wave oscillations modulate the radio emission at a frequency (in general) incommensurate with the spin period (P_1) of the pulsar. The modulated emission is manifested in the form of drifting subpulses or quasi-stationary behaviour, where the amplitudes of the individual pulses in each component are modulated in a cyclic fashion.

Clemens & Rosen (2004) only addressed the total power observations of pulsars and modelled it accordingly. Clemens & Rosen (2008) expanded the model to include polarization behaviour, specifically the two polarization modes. This included a scalar parameter, quantitatively fitted by the model to the data, which relates the intensity of the two polarization modes. The model did not address multiwavelength observations and, by default, assumed that the ratio of the strength of the two modes in the model was constant with observational frequency.

The three objections to a non-radial oscillation model discussed in Hassell II are reasonable when considering only the total power and given the limited scope of the model at a single frequency.

First, Hassell II restate that a requirement of a non-radial oscillation model is that the nodal lines should intrude subpulse phase steps of exactly 180°, as cited in Clemens & Rosen (2004). This is accurate when only considering the total power and only a single polarization mode. As shown in fig. 4 of Clemens & Rosen (2008), the ratio of the intensity of the two polarization modes can create subpulse phase jumps that are not equal to 180°. In Rosen & Demorest (2011), the fit of the non-radial oscillation model to the data produced a phase jump greater than 180°, due to the ratio of the two polarization modes. (The fact that fitting the model to the data resulted in a simulated phase jump of 187.°7 rather than a 145.°1 is because the model fits the Stokes parameters directly and the phase jump indirectly.) If we assume, in the model, that both the ratio of the two polarization modes and the sightline are constant with observational frequency, Hassell II are correct in their assumption that it is unlikely that the subpulse phase step would increase systematically with observational frequency. Yet, as shown in Figs 3 and 2, the ratio of the polarization modes does change with frequency. The combination of a change in sightline traverse with observational frequency [see the discussion in Rosen & Demorest (2011) and the Introduction of this paper] and the change in the ratio of the two polarization modes with observational frequency could produce a systematic change in subpulse phase.

From a theoretical standpoint, if we assume that the oscillations occur on the stellar surface, their polarization characteristics should be independent of observational frequency. However, any surface motion would be tied to the magnetosphere in a way that is not well understood; it is conceivable that modelling the multifrequency observations with variable amplitudes for the polarization modes does *not* rule out surface oscillations.

Secondly, Hassall II point out that a requirement of the non-radial oscillation model is that the spacing of the components should follow the distribution of a spherical harmonic sampled along the line of sight. This requirement of the model was clearly stated

in Clemens & Rosen (2004), and it was assumed that the centre of the spherical harmonic is aligned with the centre of the pulse profile. Hassall II correctly note that the size of the components in B0809+74 is equal, thus violating a requirement of the non-radial oscillation model. As the model was adapted to incorporate polarization in Clemens & Rosen (2008), it also included a 'pulse window' that is separate from the pulsation model and limits the effects of the pulsations to the regions where emission occurs (Rosen & Clemens 2008). The non-radial oscillation model initially used a Gaussian to simulate the pulse window (Rosen & Clemens 2008) but was later adapted to use the average pulse profile (Rosen & Demorest 2011). The addition of the pulse window can cause both the spacing and the width of the pulse components to deviate from a spherical harmonic. Furthermore, as discussed in the Introduction, B0809+74 possibly has an incomplete profile, which would mean that the spherical harmonic does not align with the centre of the pulse profile.

Finally, Hassall II note that the non-radial oscillation model cannot explain how the subpulse phase begins on the leading edge of the pulse profile at low frequencies and moves through to the trailing edge at high frequencies. This is only true if the change in geometry as a function of observational frequency is not considered. Low frequency emission occurs higher in the magnetosphere than the high frequency emission and on magnetic field lines that originate closer to the magnetic pole, effectively sampling a different part of the stellar surface (Smits et al. 2006). Therefore the apparent size of the nodal regions will change with observational frequency as above, and this will result in an apparent shift in the longitude of the nodal lines. As the sightline traverse nears the magnetic pole, the nodal regions become smaller, effectively moving the nodal lines in longitude. Assuming a conal geometry and a potentially incomplete pulse profile, the nodal line (and thus subpulse phase jump) could systematically change with longitude.

4 DISCUSSION

4.1 The B0809+74 carousel model

Extensive efforts were made in the preparation of Papers 1 and 2 to determine the carousel geometry and circulation time (CT) of pulsar B0809+74. Any interpretation of the emission geometry, of course, is complicated by the various incomplete (or 'absorbed') high-frequency profiles. Indeed, the 1400-MHz profile appears to be most complete (relative to higher and lower frequencies), but it is obviously not complete because it shows no edge depolarization – especially on its highly linearly polarized leading edge, making it difficult to assess the completeness of the profile. Therefore, Paper 1 gives two geometric models that made a 'narrow' and 'broad' assumption about how much of the profile is missing at 1380 MHz. What then is clear is that these bracketing models do not differ much in their values for α and β, half a degree for the former and hardly $0.^{\circ}2$ for the latter. Therefore, it can hardly be doubted that the magnetic latitude α is about 8°–9° and the impact angle β some $4.^{\circ}5$–5° for B0809+74.

With regard to determining the carousel CT, we were perhaps less successful. At first we expected the drift-modulation frequency to be highly aliased because extrapolation from B0943+10's value (Deshpande & Rankin 1999, 2001, latter hereafter DR) suggested that it could be as short as 6.4 P_1. Moreover, B0809+74 does null as was so famously studied by Lyne & Ashworth (1983) – and on the basis of the pulsar's 'memory across nulls' we sought evidence of the CT in artificial null-removed sequences. The pulsar's fluctuation spectra are of remarkably high quality and appeared more coherent when the nulls were removed. Disappointingly, though, they were devoid of features other than that of the primary modulation and a weak harmonic. Therefore, we never found indication of any CT in this manner or in more sophisticated inverse-cartographic mapping searches.

Some relief came from the pulsar's nulls, by which van Leeuwen et al. (2002, 2003) in two important papers showed that the carousel recovery after nulls indicated that the primary fluctuation frequency was not aliased – and therefore was of alias order 0. But while this implied that the CT is merely some subbeam multiple of the drift band separation P_3, it in turn raised the spectre that the CT might be very long, several hundreds of rotation periods. Using the various means described in Papers 1 and 2, we tested this possibility, and the results were that the pulsar probably has some 9/11 beams if an outside sightline traverse and roughly 25–40 if an inside traverse. This then implied that the CT could be in the range 75–90 s in the first case and 6–9.5 min in the latter one. Subbeam maps corresponding to these two possible situations, a 34-beam and a 10-beam (polarized) one for the two cases, respectively, are given in Paper 2: figs 3 and 4. With 20–20 hindsight, we have wondered if an error was made in searching for carousel 'solutions' using the null-removed sequences; however, we also relied heavily on a natural sequence of length 858 pulses that was null free.

4.2 Status of the carousel model

The carousel model in more or less the form first articulated by Ruderman & Sutherland (hereafter RS) has proven highly successful, first in understanding the structure of B0943+10's system (DR) and then the normal 11-P_1 drift of B0809+74. In the interval, further studies have strongly suggested that carousel action drives conal phenomena in many or even most pulsars (Weltevrede, Edwards & Stappers 2006; Weltevrede, Stappers & Edwards 2007). Null-related phenomena have provided further indications regarding CTs, in a few cases very reliably (e.g. Herfindal & Rankin 2007, 2009; Rankin & Wright 2008) – and we have learned how complex nulling together with fluctuation-spectral evidence can be in, for instance, the recent work on B1918+19 (Rankin, Wright & Brown 2013) – so overall, the carousel model does seem to provide both quantitative description and qualitative understanding of several related and interacting complex processes.

More to the point here, however, is to state clearly that the carousel model is yet an heuristic model that provides frustratingly little physical insight. All the measured CTs are well longer than envisioned by RS, and the partially screened revisions by Gil, Melikidze & Geppert (2003) and Gil et al. (2008) may provide better guidance, or perhaps the recent work by van Leeuwen & Timokhin (2012). The model gives little understanding about the number and spacing of the subbeam's parent 'sparks'. It provides no guidance whatsoever in understanding why the two concentric cones in double cone pulsars have phase-locked sets of drifting subpulses. It gives no explanation for why the displaced sets of modal subbeams on outer conal edges are usually displaced in magnetic longitude by half their angular separation. Finally, it provides no way to understand why only some of the rotating 'beamlets' are visible along our sightline (and in B0943+10 a varying number after B-mode onset) giving clear credence to the incomplete profile phenomenon (but not illuminating the physics) of this 'absorption'. Finally, returning specifically to B0809+74, the carousel model gives no insight into this pulsar's unique 'memory across nulls' phenomenon.

4.3 Status of the B0809+74 non-radial oscillation model

The non-radial oscillation model was first developed in Clemens & Rosen (2004, 2008) and applied to pulsar B0943+10 in Rosen & Clemens (2008). Pulsar B0809+74, despite its often precise drifting, shows more complex behaviour than B0943+10 in almost every way: polarization, profile evolutions, phase behaviour, etc. Rosen & Demorest (2011) applied the non-radial oscillation model to B0809+74 at a single frequency.

Hassall II conducted a multifrequency analysis of B0809+74 and discussed some difficulties that the non-radial oscillation model has in explaining the complex behaviour. We address these difficulties, specifically the original total power formulation of the model-exhibited difficulties that were repaired in the later papers, but their ramifications were not explicitly stated. Further, we discuss possible ways the model can be adapted for multiple frequency observation.

As this discussion demonstrates, more detailed testing of the non-radial oscillation model in the B0809+74 context proves difficult and inconclusive for many of the same reasons that frustrated assessment of the carousel model: we simply do not yet have an adequately clear model of its profile evolution and emission geometry. Both models require estimates of the magnetic axis longitude, something that the Hassall papers did not attempt, and without it little further can be determined.

Nonetheless, the non-radial oscillation model retains great appeal. It is founded on a phenomenon well known for white dwarfs and thus utterly plausible for neutron stars. Many questions remain about the excitation and driving mechanism for oscillations in neutron stars. However, by showing that a phenomenological model for oscillations in neutron stars can quantitatively reproduce the observed behaviour, we can then use our findings (such as oscillation frequency as a function of spherical degree) to assist in the development of the theoretical framework for both oscillations and how the oscillations are coupled to the emission process.

In summary, the relative successes of the carousel model have thrown its lack of any strong physical foundation into even clearer focus. Similarly, major uncertainties still remain between the appealing physical foundations of the non-radial oscillation model and its practical application. Perhaps the two approaches might support some hybrid physical model.

ACKNOWLEDGEMENTS

Portions of this work were carried out with support from US National Science Foundation Grants AST 08-07691. This work used the NASA ADS system.

REFERENCES

Bartel N., 1981, A&A, 97, 384
Bartel N. et al., 1981, A&A, 93, 85
Bruk Y. M., Ustimenko B. Y., Popov M. V., Soglasnov V. A., Novikov A. Y., 1986, Sov. Astron. Lett., 12, 381
Clemens J. C., Rosen R., 2004, ApJ, 609, 340
Clemens J. C., Rosen R., 2008, ApJ, 680, 664
Cordes J. M., 1978, ApJ, 222, 1006
Deshpande A. A., Rankin J. M., 1999, ApJ, 524, 1008
Deshpande A. A., Rankin J. M., 2001, MNRAS, 322, 438 (DR)
Deutsch A. J., 1955, Ann. Astrophys., 18, 1
Edwards R. T., 2004, A&A, 426, 677
Gil J., Melikidze G. I., Geppert U., 2003, A&A, 407, 315
Gil J., Haberl F., Melikidze G. I., Geppert U., Zhang B., Melikidze G., Jr, 2008, ApJ,, 686, 497
Hassall T. E., Stappers B. W., Hessels J. W. T., Kramer M., 2012a, A&A, 543, A66 (Hassall I)
Hassall T. E., Stappers B. W., Weltevrede P., Hessels J. W. T., 2012b, A&A, 552, A61 (Hassall II)
Herfindal J. L., Rankin J. M., 2007, MNRAS, 380, 430
Herfindal J. L., Rankin J. M., 2009, MNRAS, 393, 1391
Hobbs G., Lyne A. G., Kramer M., Martin C. E., Jordan C. A., 2004, MNRAS, 353, 1311
Lyne A. G., Ashworth M., 1983, MNRAS, 204, 519
Lyne A. G., Manchester R. N., 1988, MNRAS, 234, 477 (LM)
Lyubarski Y. E., 2008, in Bassa C., Wang Z., Cumming A., Kaspi V. M., eds, AIP Conf. Proc. Vol. 983, 40 YEARS OF PULSARS: Millisecond Pulsars, Magnetars and More. Am. Inst. Phys., New York, p. 29
Mitra D., Rankin J. M., 2011, ApJ, 727, 92
Page C. G., 1973, MNRAS, 163, 29
Popov M. V., Smirnova T. E., Soglasnov V. A., 1987, SvA, 31, 529
Ramachandran R., Rankin J. M., Stappers B. W., Kouwenhoven M. L. A., van Leeuwen A. G. L., 2002, A&A, 381, 993
Rankin J. M., 1993, ApJ, 405, 285 and A&AS, 85, 145 (ET VI)
Rankin J. M., Ramachandran R., 2003, ApJ, 590, 411
Rankin J. M., Suleymanova S. A., 2006, A&A, 453, 679
Rankin J. M., Wright G. A. E., 2008, MNRAS, 385, 1923
Rankin J. M., Ramachandran R., Suleymanova S. A., 2005, A&A, 429, 999 (Paper 0)
Rankin J. M., Ramachandran R., Suleymanova S. A., 2006a, A&A, 447, 235 (Paper 1)
Rankin J. M., Ramachandran R., van Leeuwen J., Suleymanova S. A., 2006b, A&A, 455, 215 (Paper 2)
Rankin J. M., Wright G. A. E., Brown A. M., 2013, MNRAS, 433, 445
Rosen R., Clemens J. C., 2008, ApJ, 680, 671
Rosen R., Demorest P., 2011, ApJ, 728, 156
Ruderman M., Sutherland P., 1975, ApJ, 196, 51 (RS)
Shitov Yu. P., Malofeev V. M., 1985, Sov. Astr. Lett., 11, 39
Smirnova T. V., Soglasnov V. A., Popov M. V., Novikov A. Y., 1986, SvA, 30, 51
Smits J. M., Stappers B. W., Edwards R. T., Kuijpers J., Ramachandran R., 2006, A&A, 448, 1139
Thorsett S. E., 1991, ApJ, 377, 263
van Leeuwen J., Timokhin A. N., 2012, ApJ, 752, 155
van Leeuwen J., Kouwenhoven M. L. A., Ramachandran R., Rankin J. M., Stappers B. W., 2002, A&A, 387, 169
van Leeuwen J., Ramachandran R., Rankin J. M., Stappers B. W., 2003, A&A, 399, 223
Weltevrede P., Edwards R. T., Stappers B. W., 2006, A&A, 445, 243
Weltevrede P., Stappers B. W., Edwards R. T., 2007, A&A, 469, 607

This paper has been typeset from a TEX/LATEX file prepared by the author.